

Intense switchable fluorescence in light wave coupled electrowetting devices

J. Heikenfeld^{a)}

Extreme Photonix LLC, Cincinnati, Ohio 45219-2374

A. J. Steck^{b)}

Nanoelectronics Laboratory, University of Cincinnati, Cincinnati, Ohio 45221-0030

(Received 1 September 2004; accepted 20 October 2004; published online 22 December 2004)

Switchable fluorescence has been obtained from light wave coupled (LWC) electrowetting (EW) devices fabricated on an optical waveguide substrate. The LWC device structure contains a polar water component and a nonpolar oil component that compete for placement on a hydrophobic surface under the influence of an applied electric field. The oil film contains organic lumophores that fluoresce intense red (608 nm), green (503 nm), and blue (433 nm) light with $\sim 90\%$ quantum efficiency when excited by violet light. Violet InGaN light-emitting diodes (LEDs) couple ~ 405 nm excitation light into the waveguide substrate. EW of the water layer displaces the fluorescent oil film such that it is either optically coupled to, or decoupled from, the underlying waveguide. The output luminance can be modulated from >100 cd/m² to <5 cd/m² as a dc voltage ranging from 0 to -24 V is applied to the water layer. Maximum luminance of 15×30 arrays of the devices may exceed ~ 500 cd/m² by simply increasing the output of the InGaN LEDs. © 2005 American Institute of Physics. [DOI: 10.1063/1.1842853]

Electrowetting¹ utilizes an applied electric field to modulate the contact angle of liquids on hydrophobic surfaces. In recent years, electrowetting (EW) has been applied to various microfluidic devices, including biomedical lab-on-chip,² micromechanical motors,³ variable focus lenses,⁴ convex/concave invertible lenses,⁵ fiberoptic communications switches,⁶ and reflective electronic paper displays.^{7,8} EW finds application throughout these fields since it can achieve robust and rapid (<10 ms) changes in physical position,^{2,3} optical surface curvature,^{4,5} and in displacement of oil films.⁶⁻⁸ In this letter, we report on intense switchable fluorescence achieved using light wave coupled⁹ (LWC) EW devices. For the LWC devices, EW of a water layer displaces a fluorescent oil film such that it is either optically coupled to, or decoupled from, an underlying waveguide that contains violet light for excitation. Photographs of red, green, and blue LWC devices in OFF and ON states of emission are shown in Fig. 1.

LWC devices with the structure shown in Fig. 2 were constructed on a glass substrate that also serves as large planar waveguide ($n \approx 1.46$). Throughout the subsequent description, critical optical properties and surface energy properties are given for the materials used. The lower, ground electrode consists of a ~ 50 nm 90%/10% In₂O₃/SnO₂ (ITO) film that is transparent ($>90\%$, $n \approx 1.95$) and electrically conducting (<40 Ω/\square). A ~ 1.0 - μm -thick hydrophobic insulator is deposited onto the ITO. This hydrophobic insulator film possesses a refractive index of ~ 1.5 and a surface energy of $\gamma < 20$ dynes/cm. A hydrophobic and reflecting optical cladding layer was also deposited and patterned onto the device. An example material for the cladding is a >1 - μm -thick film of DuPont Teflon® AF 2400 ($\gamma \sim 16$ dynes/cm, $n \approx 1.31$). The solid features of the device

are then completed with a hydrophilic grid ($\gamma \sim 40$ dynes/cm) formed from a photocurable polymer that is resistant to swelling or dissolving in oils. The hydrophilic grid lines are ~ 150 μm wide, ~ 40 μm thick, and define an individual LWC device which is $\sim 1 \times 3$ mm in perimeter. A few tenths of milliliters of deionized water (>16 M Ω cm, $n \approx 1.33$) are then dosed over the LWC array and a bias electrode wire is placed into the water layer. Next, ~ 100 to ~ 300 nL of fluorescent oil is inserted into each LWC device, forming an oil layer thickness in the tens of micrometers. The specialized oil has a surface tension of ~ 27 dynes/cm, causing it to form a continuous film positioned between the water (~ 73 dynes/cm) and hydrophobic insulator (<20 dynes/cm). This vertically layered geometry is due to interfacial surface tension relationships.¹⁰ The oil is confined laterally by the hydrophilic grid, which effectively isolates the oil in each individual device by strongly attracting the water. Interfacial surface tension forces dominate

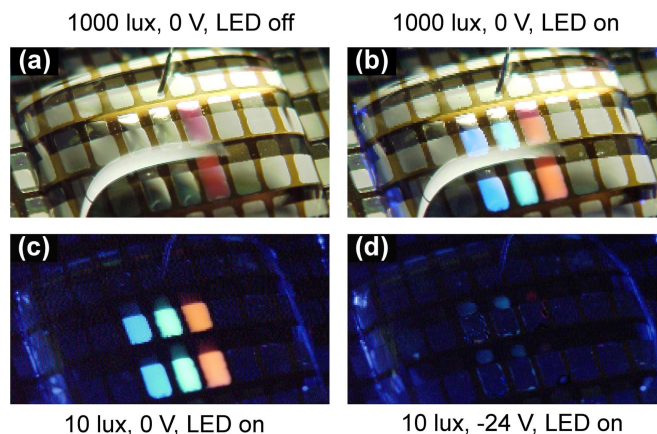


FIG. 1. (Color online) Full-color LWC devices operating under 1000 lux (a), and (b), and 10 lux (c) and (d) ambient lighting conditions: (a) violet pump off, 0 V; (b) and (c) violet pump on, 0 V; (d) violet pump on, -24 V.

^{a)}Electronic mail: jheikenf.extremephotonix@biostart.org

^{b)}Electronic mail: a.steckl@uc.edu

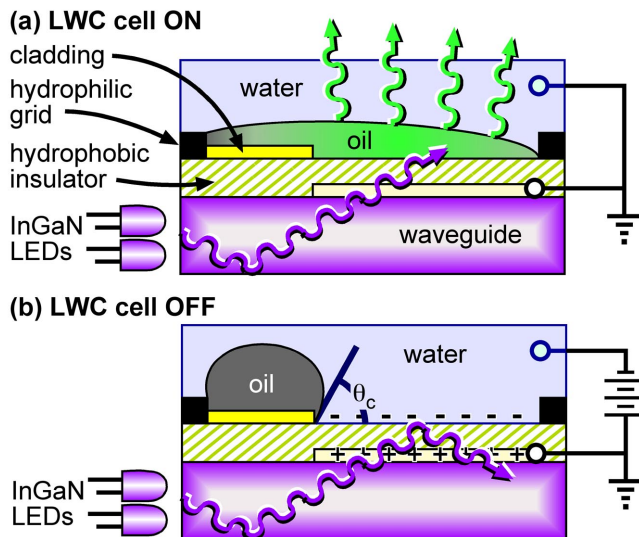


FIG. 2. (Color online) LWC device structure in the ON (a) and OFF (b) states of emission. In the ON state, violet light from the waveguide excites lumophores in the oil layer, thereby causing fluorescence.

over gravitational forces since the density of the oil is $\sim 80\%$ of the density of the water. The oil has a refractive index of ~ 1.46 , which matches it to the index of waveguide substrate. The oil is fluorescent since it contains ~ 1 wt % of red, green, or blue (RGB) nonpolar organic lumophores that fluoresce when they absorb shorter wavelength light. Lensed violet (~ 405 nm) InGaN light-emitting diodes (LEDs) with a 30° emission half-angle were optically coupled to one edge of the waveguide. Edges of the waveguide without LEDs were mirrored with Al to reflect and therefore to recycle propagation of violet light in the waveguide.

The completed LWC device structure shown in Fig. 2 is operated as follows. Violet light is coupled at an incidence angle θ_{LED} into the edge of the waveguide. This violet light then propagates within the waveguide ($n_{sp} \sim 1.46$) via internal reflection. Violet light also propagates in all layers contacting the waveguide that have refractive indices greater than or equal that of the waveguide. Layers meeting this criteria for propagation include the ITO electrode ($n \approx 1.95$), the hydrophobic insulator ($n \approx 1.5$), and the fluorescent oil layer ($n \approx 1.46$). Under conditions of zero applied bias [Fig. 2(a)] to the water layer, interfacial surface tensions cause the fluorescent oil to form a continuous film between the water and hydrophobic layers. In this configuration, violet light from the waveguide propagates through the ITO and the hydrophobic insulator, and penetrates the fluorescent oil layer. The fluorescent oil then absorbs the violet light and fluoresces with $\sim 90\%$ quantum efficiency. This results in an LWC device in the ON state [Fig. 1(b) Fig. 1(c), Fig. 2(a)].

Violet light propagation in the waveguide is governed by Snell's law of refraction at the interface between two media of refractive indexes n_1, n_2 :

$$n_1 \sin \theta_1 = n_2 \sin \theta_2 \quad \text{or} \quad n_x = \sqrt{n_w^2 - \sin^2 \theta_{LED}}, \quad (1)$$

where θ_{LED} is the LED emission half-angle at half-power and n_x is the refractive index of a material in contact with the surface of the waveguide (n_w). Given a θ_{LED} of less than 30° , violet light in the waveguide will be internally reflected by any low refractive index layer ($n_x < 1.37$). To achieve total internal reflection, a low refractive index layer must also be

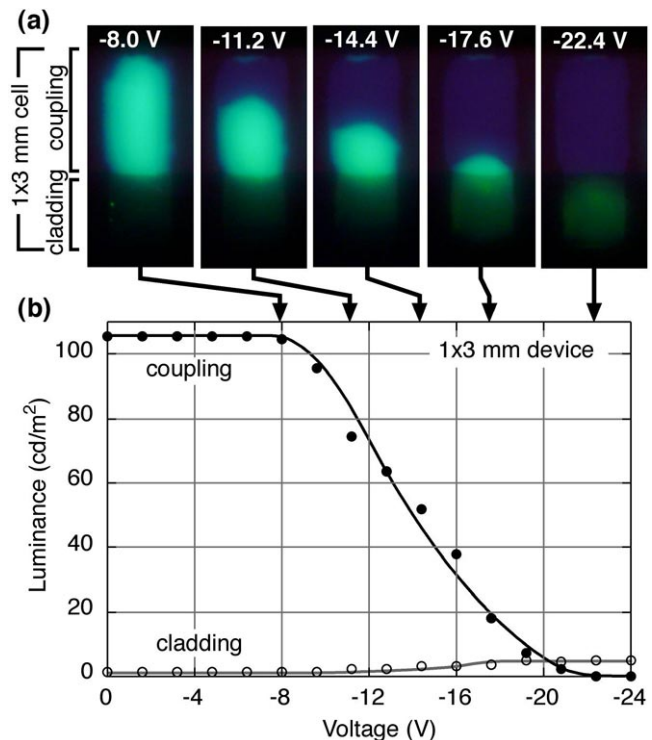


FIG. 3. (Color online) Photographs (a) of green LWC devices vs applied voltage and plot (b) of green LWC device luminance vs voltage. The LWC device luminance is separated into cladding and coupling region contributions that were weighted against their respective emitting areas in order to plot their contribution to the overall 1×3 mm device luminance.

$\geq 1 \mu\text{m}$ thick. This thickness is needed since the evanescent portion of the propagating violet light penetrates (with exponential intensity decay) $\sim 1 \mu\text{m}$ into the low refractive index layer. LWC operation utilizes this effect of total internal reflection to turn the device OFF.

As shown in Fig. 2(b) the fluorescence emission from the LWC device is switched OFF via EW. As voltage is applied to the water it is electrostatically attracted toward the hydrophobic insulator. This displaces the fluorescent oil layer onto the solid cladding layer. The cladding layer has a low refractive index of ~ 1.3 , which causes internal reflection at the cladding/hydrophobic insulator interface. The water also has a low refractive index of $n_x \approx 1.33$, which causes violet light to be internally reflected at the water/hydrophobic insulator interface. Together, the water and cladding layers reflect light internally across the entire LWC device area. Therefore, in this device configuration no optical path exists that would allow violet light to reach the fluorescent oil layer. In this OFF state, not only is fluorescence from the oil prevented, but additionally violet light is recycled back into the waveguide for use in other LWC devices in the ON state.

The luminance–voltage characteristics of the LWC device are shown in Fig. 3(b). Modulating the applied voltage induces EW and controls the amount of violet light coupled into the fluorescent oil. The applied voltage capacitively charges the surface of the hydrophobic insulator and therefore decreases the interfacial surface energy (i.e., increases attraction) between the water and hydrophobic insulator. The increased contact area of the water to the hydrophobic insulator can be predicted from the water contact angle. The water contact angle [θ_c , Fig. 2(b)] is found at the common contact point for the oil, water, and hydrophobic insulator. At

zero or constant applied voltage, interfacial surface tensions are balanced at this common point (Young's equation). Young's equation can be combined^{4,10} with Lippman's equation, which predicts a decrease in interfacial surface tension with increase in surface charge density (applied voltage). This combination results in the EW equation

$$\cos \theta_C = \cos \theta_0 + \frac{\epsilon_0 \epsilon_r (V)^2}{2z\gamma_i}, \quad (2)$$

where θ_0 is the contact angle without applied bias, V is the applied bias, ϵ_r and z are the relative dielectric constant and thickness of the hydrophobic insulator, respectively, and γ_i is the interfacial surface tension between the water and fluorescent oil.

The luminance–voltage characteristics can be separated into coupling and cladding components that are geometrically defined in Fig. 3(a). The coupling luminance corresponds to luminance contribution from device area where there is no solid cladding layer. The remaining device area contains the solid cladding layer and produces the cladding luminance contribution. At low voltage, the fluorescent oil completely covers the pixel resulting in a coupling luminance of $>100 \text{ cd/m}^2$. At a voltage of -8 V , the oil begins to be displaced onto the cladding and the luminance decreases, reaching full displacement and zero coupling luminance at -22 V . Interestingly, as the negative bias is increased, the smaller (and undesirable) cladding luminance increases to $\sim 5 \text{ cd/m}^2$. We have determined that the cladding layer itself is almost perfectly effective at reflecting incident violet light back into the waveguide. Therefore, another explanation is required for the cladding luminance. According to Eq. (1) and neglecting diffuse scattering effects, it can be estimated that if $n_x=1.33$ for water then $\sim 5\%$ of violet light from the LED is introduced into the waveguide at an angle of $>37^\circ$. The cladding luminance is therefore attributed to violet light refraction from the waveguide into the water and penetration into the fluorescent oil layer. The cladding luminance reduces the device ON/OFF contrast ratio to $\sim 20:1$. Contrast values on the order of $>100:1$ are likely achievable by selectively suppressing large angle violet light propagation in the waveguide and/or by utilizing side-emitting LED packages that emit 80% of light intensity within $\pm 20^\circ$.

The $1 \times 3 \text{ mm}$ devices currently exhibit ON/OFF and OFF/OFF switching times of $<100 \text{ ms}$. Preliminary results with smaller geometry devices indicate switching times of $\sim 10 \text{ ms}$, allowing the use of LWC devices as pixels in full-color video rate display applications. As shown in Fig. 4, LWC devices can achieve saturated RGB emissions by simply changing the lumophore introduced into the oil. Violet light excitation at $\sim 400 \text{ nm}$ is preferable over ultraviolet light since: (1) it provides a gentle excitation source that does not photodegrade the lumophores and (2) the optical components of the device are highly transparent to light at this wavelength. Waveguide materials such as polymethyl-

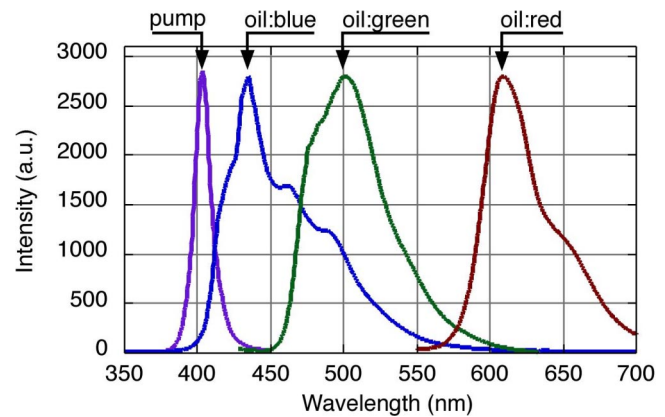


FIG. 4. (Color online) Intensity vs wavelength for LWC devices utilizing fluorescing oils containing $\sim 1 \text{ wt } \%$ RGB lumophores. Emission from the InGaN violet LED pump is also shown.

methacrylate exhibit a very low optical absorption of $<0.1 \text{ dB/cm}$ at $\sim 400 \text{ nm}$. This allows light to propagate in the waveguide over distances of $\sim 30 \text{ m}$ before 50% attenuation. This propagation efficiency along with LWC device efficiency has the potential⁹ to provide luminous efficiencies of $>10 \text{ lm/W}$ for a completed LWC display panel. Furthermore, LWC device luminance is determined primarily by the power of the violet light source. By simply increasing the InGaN LED light intensity, luminance $>500 \text{ cd/m}^2$ has been measured from 15×30 arrays of LWC devices.

In summary, we have reported switchable fluorescence achieved from LWC devices. The devices are fabricated onto a large planar waveguide substrate that is edge-pumped with InGaN violet LEDs. The LWC devices are switched via EW such that light is either selectively coupled to a fluorescent oil layer or is reflected and recycled back into the waveguide. LWC devices exhibit a switching contrast of $>20:1$, switching speeds of $<100 \text{ ms}$, RGB emission, $>500 \text{ cd/m}^2$ luminance, and 0 to -24 V operation. Further device improvements can be achieved by modifying the device geometry and the angles at which violet light propagates within the waveguide.

The authors would like to thank S. Allen for assistance in lumophore characterization.

¹C. Quilliet and B. Berge, *Curr. Opin. Colloid Interface Sci.* **6**, 34 (2001).

²M. G. Pollack, R. B. Fair, and A. D. Shenderov, *Appl. Phys. Lett.* **77**, 1725 (2000).

³J. Lee and C. Kim, *J. Microelectromech. Syst.* **9**, 171 (2000).

⁴B. Berge and J. Peseux, *Eur. Phys. J. E* **3**, 159 (2000).

⁵S. Kuiper and B. H. W. Hendriks, *Appl. Phys. Lett.* **85**, 1128 (2004).

⁶P. Mach, T. Krupenkin, S. Yang, and J. A. Rogers, *Appl. Phys. Lett.* **81**, 202 (2002).

⁷R. A. Hayes and B. J. Feenstra, *Nature (London)* **425**, 383 (2003).

⁸T. Roques-Carnes, R. A. Hayes, B. J. Feenstra, and L. J. M. Schlangen, *J. Appl. Phys.* **95**, 4389 (2004).

⁹J. Heikenfeld and A. J. Steckl, *Proc. Soc. Inf. Display*, Seattle, 2004, Vol. 35, p. 470, ISSN-0004-966X.

¹⁰B. Janocha, H. Bauser, C. Oehr, H. Brunner, and W. Göpel, *Langmuir* **16**, 3349 (2000).